

Current Biology

A combination of pollen mosaics on pollinators and floral handedness facilitates the increase of outcross pollen movement

Highlights

- Reciprocal handedness in plants (enantiostyly) leads to outcrossing
- Left and right morphs place most of their pollen on different sides of pollinators
- Spatial mosaics of pollen quality were found on each side of pollinators
- Exploitation of mosaics increases outcrossing beyond expectations of enantiostyly

Authors

Corneile Minnaar, Bruce Anderson

Correspondence

banderso.bruce@gmail.com

In brief

Minnaar and Anderson use quantum dots to track pollen movement in a handed plant. Outcrossing is higher than expected because stigmas are positioned to preferentially pick up pollen from outcross-pollen hotspots on each side of pollinators. This positional pollen discrimination could be considered a kind of female choice in plants.

Report

A combination of pollen mosaics on pollinators and floral handedness facilitates the increase of outcross pollen movement

Corneile Minnaar¹ and Bruce Anderson^{1,2,3,*}

¹Department of Botany and Zoology, Stellenbosch University, Stellenbosch, South Africa

²Twitter: @BioInteractLab

³Lead contact

*Correspondence: banderso.bruce@gmail.com

<https://doi.org/10.1016/j.cub.2021.04.074>

SUMMARY

Darwin devoted an entire book to style and stamen polymorphisms, exemplifying the importance of pollen movement efficiency as a selective agent on floral form.¹ However, after its publication, his interest was piqued by a description of floral handedness² or enantiostyly.³ Todd² described how left- and right-handed *Solanum rostratum* flowers have styles deflected to the left and right, respectively. Darwin⁴ wrote to Todd for seeds so that he could "...have the pleasure of seeing the flowers and experimenting on them," but he died just days later on 19 April 1882. More than a century elapsed before the first experiments demonstrated that handedness leads to high rates of outcrossing.^{5,6} By attaching quantum dots to pollen grains, we tracked pollen movement in *Wachendorfia paniculata*, which has one stamen on the same side of the style and two deflected in the opposite direction. We found that handedness leads to outcrossing because left- and right-handed morphs place most of their pollen on different sides of the pollinators. However, the partial separation of stamens and style also results in two-dimensional pollen quality mosaics on each side of carpenter bee pollinators, generating hotspots and coldspots of outcrossed pollen. Similar mosaics were not found on honeybee pollinators. Outcrossed pollen receipt was much higher than expected because stigmatic positions are fine-tuned to match the outcross pollen hotspots on carpenter bees. Exploitation of these pollen mosaics enables plants to increase the probability of between-morph (i.e., disassortative), outcross pollen movement beyond the expectations of enantiostyly.

RESULTS AND DISCUSSION

While a dearth in technology has made quantifications of pollen movement one of the least-studied aspects of pollination,^{7,8} high outcrossing rates in handed plants suggest that handedness reduces pollen movement within multi-flowered plants.^{5,6} Negative fitness costs associated with pollen movement within plants (e.g., inbreeding and incompatibility issues) are thought to have driven widespread spatial separation of anthers and stigmas across many angiosperm families.⁹ However, the spatial separation of stigmas and anthers introduces a novel cost: pollen transfer efficiency is reduced because stigma-anther separation increases the distance between pollen placement and receipt sites.^{10,11} Reciprocally handed plants elegantly resolve this conundrum—left-handed flowers place most of their pollen on the left sides of pollinators where they are picked up by right-handed flowers, while right-handed flowers do exactly the opposite¹¹ (Figure 1A). Consequently, most mating is thought to occur between morphs (disassortative mating), rather than within morphs (assortative mating). The reciprocity of left- and right-handed flowers thus maintains the efficiency of outcross pollen transfer while allowing stigma-anther separation to reduce pollen movement within plants.^{11–13}

In fact, handedness or enantiostyly comes in many forms:¹⁴ numerous enantiostylous species such as *Solanum rostratum* have several central feeding anthers and a single, large cryptically colored anther deflected in the opposite direction to the style; some only produce pollen as rewards while others produce nectar; in some, all flowers on a plant are the same morph (dimorphic enantiostyly), while in others, both left- and right-hand morphs occur on the same plant (monomorphic enantiostyly). In theory, for all enantiostyly, outcrossing should be maximized when all of the stamens and styles on a plant are deflected in opposite directions (Figure 1A). However, in monomorphic enantiostyly, styles and stamens of different flowers can face the same direction, leading to self-pollen transfer.⁵ Similarly, individual flowers of many entiostylous plants can have some stamens on the same side as the style (e.g., all handed Haemodoraceae, the family in which handedness is most prevalent,¹⁵ and some Commelinaceae¹⁴). *Wachendorfia paniculata* Burm. (Haemodoraceae) has two stamens opposing the style and one that occurs on the same side (Figure 1B). All three *W. paniculata* anthers have the same number of pollen grains;¹⁶ thus, perfect left-right segregation in pollen placement by this 2:1 stamen arrangement is expected to result in approximately 66.7% between-morph pollen movement (Figure 1B). However, between-morph

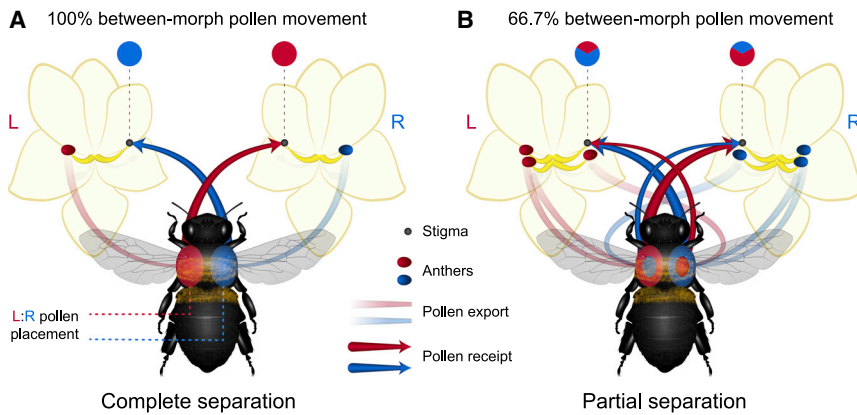


Figure 1. Comparing the theoretical efficiency of pollen movement in dimorphically enantiostylous plants (entire plants are either left- or right-handed), where anthers and stigmas are completely separated versus partially separated, assuming perfect left-right segregation in pollen placement and receipt

(A) Complete stigma-anther separation: pollen from the left and right morph is placed on the right and left sides of the pollinator's body, respectively. Stigmas from left and right morphs make contact with separate sides of pollinator bodies and therefore only capture pollen from opposite morphs, resulting in 100% between-morph pollen movement.

(B) Partial separation: between-morph pollen movement is reduced because flowers place

some of their pollen on the same side as stigmas, causing within-morph pollen movement. In this example (as in *Wachendorfia paniculata*), two stamens are opposite to the style while one stamen remains on the same side, resulting in maximum expected between-morph pollen movement of 66.7%.

pollen movement is likely to be much lower than 66.7% if grooming and leg/wing movement reposition pollen after it is placed on the pollinator, or if the angle of approach by pollinators is very inconsistent.

Despite this, *W. paniculata* appears to outcross much more effectively than predicted (range: 0.78–0.98).¹⁷ Since self-pollinated *W. paniculata* flowers set fewer seeds than outcrossed flowers,¹⁷ it is unclear how much the high outcrossing rates (determined using mature seeds) reflect the mechanics of non-random pollen movement versus the reduced developmental

success of self-fertilized ovules. We use fluorescent semiconductor nanocrystals (quantum dots) to directly quantify *W. paniculata* pollen movement.

We captured honeybees (*Apis mellifera capensis*) and carpenter bees (*Xylocopa caffra*) visiting flowers with quantum-dot-labeled pollen and mapped the positions of labeled pollen on pollinators. Pollen was placed on the beating wings and sometimes the flanks of bees as they approached and landed on flowers (Figure S1; Video S1). Partial separation of styles and stamens results in strong segregation of pollen on pollinators, a

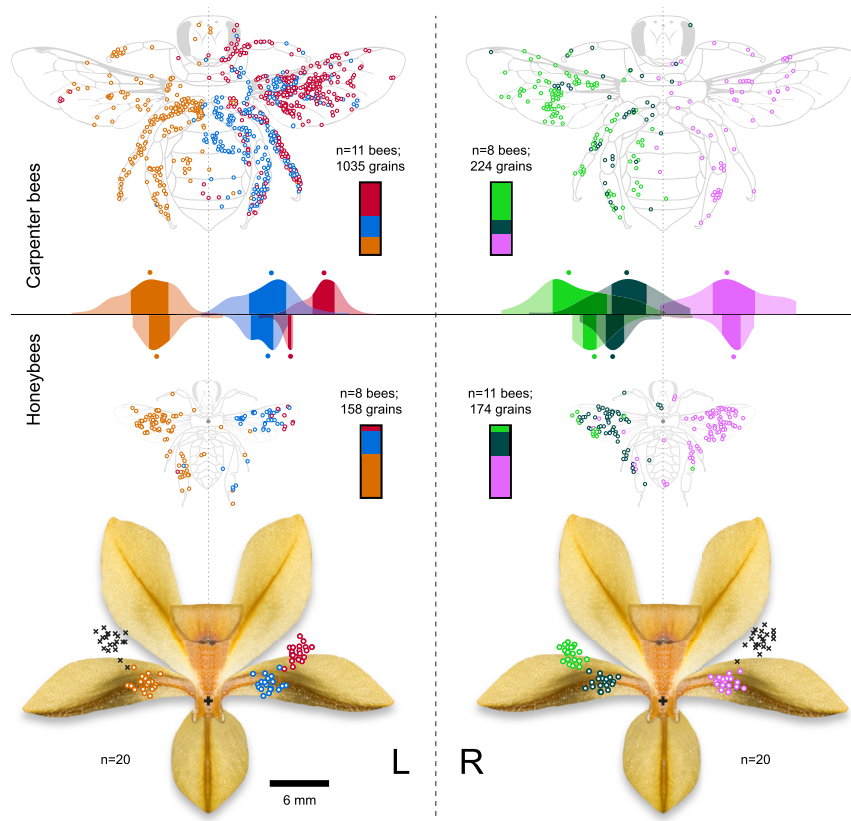


Figure 2. Scale drawing showing the positions of floral reproductive parts with colors that correspond to the positions of pollen found on captured honeybee and carpenter bee pollinators

Left- and right-handed flowers are shown from behind so that pollinators can be visualized in a position of approach, where black crosses = stigmas and colored dots = anthers. Half-violin plots show the pollen placement distribution along the x axis (L–R) on carpenter bees and honeybees for both morphs. Darker portions of violin plots represent the inter-quartile range and dots above distributions indicate the median. Bars show the proportion of pollen placed on bees from each anther. See also Figure S1, which shows a photograph of a carpenter bee (*Xylocopa caffra*) wing and body (4× magnification) after making contact with a quantum dot labeled flower. Statistical differences in positions of floral parts can be found in Table S1. Statistical differences in the positions of pollen placement by different anthers can be found in Table S2. See also Video S1, which shows slow-motion footage of pollinators making contact with anthers.

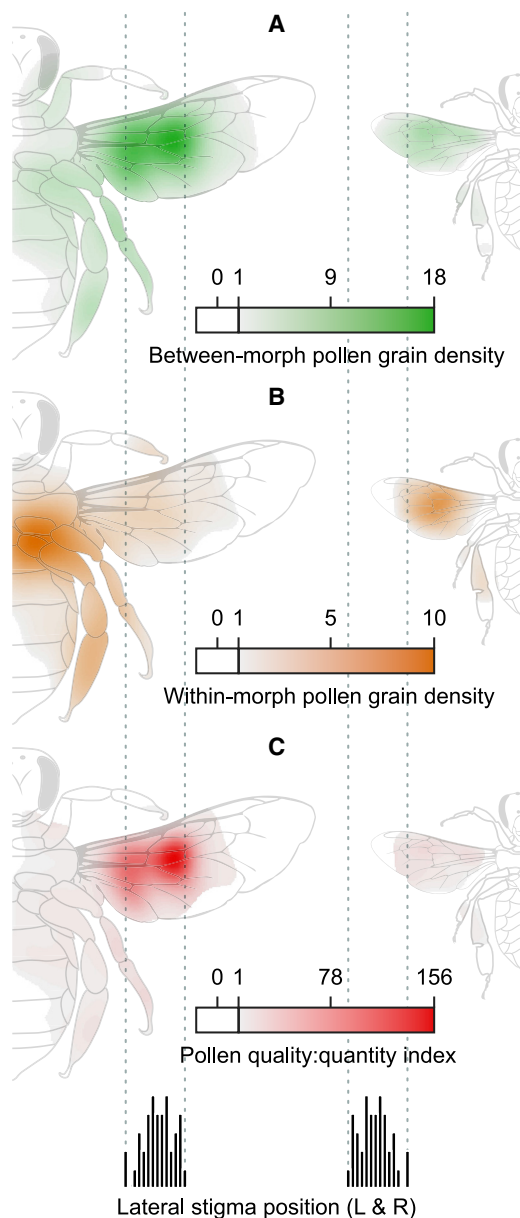


Figure 3. Heatmaps combining pollen placement from left- and right-handed flower morphs for carpenter bees and honeybees

Right, carpenter bees; left, honeybees. Heatmaps show (A) between-morph pollen density (pollen grains per 0.1 mm² grid cell), (B) within-morph pollen density (pollen grains per 0.1 mm² grid cell), and (C) pollen quality–quantity (between-:within-morph pollen grain ratio × total number of grains). White areas in heatmaps represent areas where pollen density was close to zero. Dotted gray lines show the combined lateral range of left and right stigmas relative to flower central axes and plotted relative to bee body central axis. Black bars show the frequency distribution of lateral stigma positions within the total stigma range.

prerequisite for enantiostyly to generate non-random pollen movement between morphs (Figure 2).

An unforeseen result was that small differences in upper and lower anther positions (Figure 2; Table S1) translate into clearly different pollen placement sites (Figure 2; Table S2). While lower

anthers placed pollen primarily on the flanks of carpenter bees, upper anthers placed pollen closer to the wing tips (Figure 2) and constituted the bulk of wing pollen (69.3%). Pollen from the upper anthers was seldom deposited on honeybees as their out-stretched wings are too short to consistently contact the upper anthers. Consequently, most labeled pollen on honeybees originated from the lower anthers of both morphs (Figure 2).

An important consequence of site-specific pollen placement by different anthers (Figure 2) is that it results in predictable mosaics in pollen quality on pollinators. Between- and within-morph pollen transfer differs in terms of average pollen grain quality: pollen movement within morphs can include pollen movement within a plant (geitonogamous, self-pollen), and for *W. paniculata*, this results in reduced seed set.^{16,17} In contrast, pollen movement between morphs has no low-quality self-component. The asymmetric anther arrangement of *W. paniculata* means that lower anthers always have a positional match on the opposite morph while upper anthers do not. Consequently, stigmatic contact with lower-anther placement sites is likely to result in equal mixtures of within- and between-morph pollen. In contrast, stigmatic contact nearer the wing tips should result in mostly between-morph pollen receipt from the unmatched upper anthers. To quantify pollen quality variation on pollinators, we created pollen quality heatmaps (Figure 3). These maps provide evidence of pollen quality mosaics on pollinators. Large quantities of mostly between-morph pollen were found in the middle of carpenter bee wings whereas an even mixture of between- and within-morph pollen was found closer to the midline of the carpenter bees. There were no clear between-morph pollen “hotspots” on honeybees because labeled pollen on honeybees was mostly from the matched lower anthers.

If *W. paniculata* stigmas are positioned to make more frequent contact with the between-morph pollen hotspots on carpenter bee wings than with the mixed quality loads on carpenter bee flanks and honeybee wings, then we would expect pollen movement between morphs to exceed the 66.7% predicted by the 2:1 anther arrangement. We measured stigma positions during peak pollinator activity (9:00–12:00) and found that stigmas were positioned significantly higher and wider than the upper anthers (Figure 2; Table S1), suggesting their position is not a precise match to upper anthers. Instead of matching the upper anther positions, stigma positions appear to match areas with the highest proportions of high-quality pollen, rather than simply high numbers of grains (Figure 3).

Indeed, we found (Figure 4) that 75.9% of pollen on left-handed stigmas was from the opposing right-handed anthers (right-handed stigmas received 73.4% of their pollen from the opposing left-handed stigmas; Figures S2 and S3). While the lower anther opposite to the stigma contributed mostly to the opposite morph (90.46%), their overall contribution (i.e., 8.8% of pollen on the stigmas of left-handed flowers) was far less than the upper anthers. While the lower, stigma-side anthers contributed most pollen to their own morph (90.09%), only 12.8% of all pollen found on left-handed stigmas was from the stigma-side anther. The slight mismatch in stigma-anther position skews pollen receipt toward upper anthers (Figure 4), resulting in very strong between-morph pollen movement overall (85.81% left and 86.41% right)—significantly higher than the

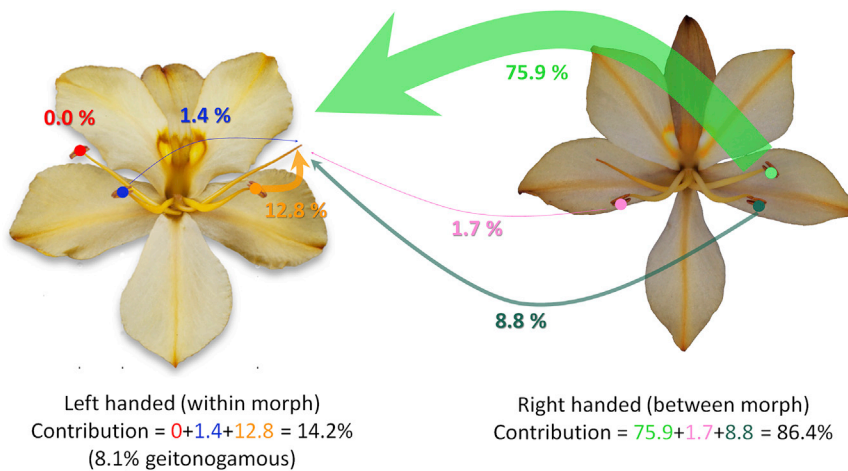


Figure 4. Relative pollen contributions made by different anthers to the stigmas of the left-handed *W. paniculata* morph

Arrow thickness is proportional to the percentages of labeled pollen found on the stigma. By adding these different values, one can see that 86.4% of labeled pollen found on left-handed stigmas is from the opposing right-handed morph. 14.2% of all pollen found on left-handed stigmas was from the left-handed morph and a separate experiment determined that 8.1% of all pollen found on stigmas was geitonogamous in origin (more than half of the within-morph contribution). Note that this figure only shows pollen receipt by the left-handed morph. We show the reciprocal figure (pollen receipt by the right-handed morph) in Figure S2. Replication of this experiment is visualized in Figure S3, demonstrating the low level of variability found between replicates and across morphs.

66.7% initially predicted ($\chi^2 = 178.82$, $df = 1$, $p < 0.005$). This also translated to low proportional receipt of geitonogamous pollen ($8.08\% \pm 4.81\%$ SD, $n = 12$), explaining the higher than expected rates of outcrossing previously measured in populations of *W. paniculata*.¹⁷ A similar study¹⁸ was conducted on distylous primroses, which have two floral morphs differing in the reciprocal arrangement of style and stamen height. Using differences in pollen size, the authors were also able to show how reciprocal style and stamen polymorphisms resulted in differential pollen placement on different parts of the pollinator and consequently high outcross pollen movement. These complementary results suggest that distyly and enantiostyly are similarly functioning mechanisms that increase outcrossing rates and the efficiency of pollen transfer.

While this manuscript suggests that handedness clearly evolved to promote efficient outcross pollen movement between morphs (similar to distyly¹⁸), pollen discrimination also suggests the possibility of female choice in plants. If sexual selection is considered as the selection for traits that increase mating success rather than survival,¹⁹ then stylar traits that confer higher incidences of outcrossing could be considered products of sexual selection because they are likely to lead to more successful matings and do not increase the survival of the parent plants. In plants, sexual selection via female choice is usually only considered to occur long after mating (e.g., through selective abortion of fertilized ovules).¹⁹ However, *W. paniculata* (and other heterostylous plants¹⁸) appears capable of using pollen position as a rough surrogate for quality, and we present evidence that stigmas harvest pollen primarily from high-quality hotspots on pollinators, suggesting that forms of mate selection can take place prior to or during mating. There are, however, many striking differences between the apparent choices made by *W. paniculata* and the kinds of choices made by animals: animals typically make active choices based on the phenotypes of individuals, but *W. paniculata* plants make “passive” choices based on the positions of pollen grains; in a single mating event, animals mate with a much smaller subset of the population (i.e., 1 individual) than plants (plants can receive many pollen grains of mixed parentage); *W. paniculata* discriminate only against self-matings, whereas animals discriminate against a plethora of

phenotypic traits; and the choices made by animals can lead to the evolution of secondary sexual traits like attractiveness. In contrast, the “choices” described here are unlikely to lead to increased floral attractiveness but may select on phenotypic traits that control the precision of pollen placement and receipt. While plants are often viewed as relatively passive participants in their own mating process, this manuscript suggests that plants may nevertheless possess rudimentary mate discrimination capabilities. Although sexual selection through male competition in plants is now widely accepted, Darwin did not consider it a possibility in plants,¹⁹ and given the available evidence, it is uncertain whether he would have contested or accepted the idea of female choice in plants.

Given that handedness primarily evolved to promote outcross pollen movement, it seems pertinent to ask why partial style-stamen separation is so prevalent in enantiostylous plants and why the lower anthers in *W. paniculata* have been retained. One cost of complete style-stamen separation is that it limits the pool of possible mates in a population by 50%, and this may be especially detrimental in very small populations. Partial style-stamen separation reduces this cost because the anthers on both sides allow matings to occur between all individuals within a population. This advantage of the stigma-side anther is made possible by the fact that different morphs are compatible; however, any inbreeding depression resulting from self-pollination in *W. paniculata*^{16,17} is likely to reduce the advantage of having a stigma-side anther. Clearly, the rates of self-pollen movement ($\sim 8\%$) and inbreeding depression in *W. paniculata* are not high enough to outweigh the advantages of having a stigma-side anther. The arrangement of anthers and stigmas in *W. paniculata* may also represent various bet-hedging strategies⁸ to ensure that male and female function can contribute to overall plant fitness in a variety of pollination environments. For example, when carpenter bees visit flowers often, pollen movement will be dominated by upper anthers and result mostly in outcrossing. However, when honeybees are the most frequent visitors, or when morph ratios are highly skewed (e.g., during colonizing events), pollen movement will likely be dominated by lower anthers, leading to reduced outcrossing, but with increased reproductive assurance relative to theoretical flowers only possessing upper anthers.

STAR★METHODS

Detailed methods are provided in the online version of this paper and include the following:

- KEY RESOURCES TABLE
- RESOURCE AVAILABILITY
 - Lead contact
 - Materials availability
 - Data and code availability
- EXPERIMENTAL MODEL AND SUBJECT DETAILS
- METHOD DETAILS
 - Quantum dot application
 - Pollen placement on pollinators
 - Pollen movement
 - Stigma and anther positions
- QUANTIFICATION AND STATISTICAL ANALYSIS
 - Pollen placement on pollinators
 - Pollen movement
 - Pollen placement heatmaps
 - Stigma and anther positions

SUPPLEMENTAL INFORMATION

Supplemental information can be found online at <https://doi.org/10.1016/j.cub.2021.04.074>.

ACKNOWLEDGMENTS

The authors thank Spencer Barrett, Steve Johnson, Lawrence Harder, James Thomson, and Jeremy Midgley for comments on early drafts. Work was supported by the National Research Foundation (South Africa) (105987 to B.A. and C.M.; 111979 to C.M.), the Eva Crane Trust (ECTA_20170609 to C.M.), and British Ecological Society (EA20/1196 to B.A.).

AUTHOR CONTRIBUTIONS

The manuscript was jointly conceived by both authors. Both authors collected field data. All lab work and statistical analysis was completed by C.M. The manuscript was co-written by both authors.

DECLARATION OF INTERESTS

The authors declare no competing interests.

Received: February 18, 2021

Revised: March 24, 2021

Accepted: April 28, 2021

Published: May 26, 2021

REFERENCES

1. Darwin, C. (1877). *The Different Forms of Flowers on Plants of the Same Species* (John Murray).
2. Todd, J.E. (1882). On the flowers of *Solanum rostratum* and *Cassia chamaecrista*. *Am. Nat.* 16, 281–287.
3. Knuth, P. (1906). *Handbook of Flower Pollination* (Clarendon).
4. Darwin, C. (1887). In *The Life and Letters of Charles Darwin Including an Autobiographical Chapter*, F. Darwin, ed. (John Murray).
5. Jesson, L.K., and Barrett, S.C.H. (2002). Solving the puzzle of mirror-image flowers. *Nature* 417, 707.
6. Jesson, L.K., and Barrett, S.C.H. (2005). Experimental tests of the function of mirror-image flowers. *Biol. J. Linn. Soc. Lond.* 85, 167–179.
7. Minnaar, C., Anderson, B., de Jager, M.L., and Karron, J.D. (2019). Plant-pollinator interactions along the pathway to paternity. *Ann. Bot.* 123, 225–245.
8. Anderson, B., and Minnaar, C. (2020). Illuminating the incredible journey of pollen. *Am. J. Bot.* 107, 1323–1326.
9. Webb, C.J., and Lloyd, D.G. (1986). The avoidance of interference between the presentation of pollen and stigmas in angiosperms. II. Herkogamy. *New. Zeal. J. Bot.* 24, 163–178.
10. Barrett, S.C.H. (2002). The evolution of plant sexual diversity. *Nat. Rev. Genet.* 3, 274–284.
11. Jesson, L.K., Barrett, S.C.H., and Day, T. (2003). A theoretical investigation of the evolution and maintenance of mirror-image flowers. *Am. Nat.* 161, 916–930.
12. Barrett, S.C.H., Jesson, L.K., and Baker, A. (2000). The evolution and function of stylar polymorphisms in flowering plants. *Ann. Bot.* 85, 253–265.
13. Barrett, S.C.H. (2002). Sexual interference of the floral kind. *Heredity* 88, 154–159.
14. Jesson, L.K., and Barrett, S.C.H. (2003). The comparative biology of mirror-image flowers. *Int. J. Plant Sci.* 164, S237–S249.
15. Simpson, M.G. (1990). Phylogeny and classification of the Haemodoraceae. *Ann. Miss. Bot. Gard.* 77, 722–784.
16. Ornduff, R., and Dulberger, R. (1978). Floral enantiomorphy and the reproductive system of *Wachendorfia paniculata* (Haemodoraceae). *New Phytol.* 80, 427–434.
17. Jesson, L.K., and Barrett, S.C.H. (2002). Enantiostyly in *Wachendorfia* (Haemodoraceae): the influence of reproductive systems on the maintenance of the polymorphism. *Am. J. Bot.* 89, 253–262.
18. Keller, B., Thompson, J.D., and Conti, E. (2014). Heterostyly promotes disassortative pollination and reduces sexual interference in Darwin's primroses: evidence from experimental studies. *Funct. Ecol.* 28, 1213–1425.
19. Moore, J.C., and Pannell, J.R. (2011). Sexual selection in plants. *Curr. Biol.* 21, R176–R182.
20. Helme, N., and Linder, H.P. (1992). Morphology, evolution and taxonomy of *Wachendorfia* (Haemodoraceae). *Bothalia* 22, 59–75.
21. R Development Core Team (2008). R: A language and environment for statistical computing (R Foundation for Statistical Computing).
22. Adobe Systems (2017). Adobe Illustrator CC.
23. Minnaar, C., and Anderson, B. (2019). Using quantum dots as pollen labels to track the fates of individual pollen grains. *Methods Ecol. Evol.* 10, 604–614.
24. Minnaar, C., de Jager, M.L., and Anderson, B. (2019). Intraspecific divergence in floral-tube length promotes asymmetric pollen movement and reproductive isolation. *New Phytol.* 224, 1160–1170.
25. Pinheiro, J.C., Bates, D.M., DebRoy, S.D., and Sarkar, D. (2017). NIme: linear and nonlinear mixed effects models. R package version 3, pp. 1–131.
26. Hothorn, T., Bretz, F., and Westfall, P. (2008). Simultaneous inference in general parametric models. *Biom. J.* 50, 346–363.
27. Venables, W.N., and Ripley, B.D. (2002). *Modern Applied Statistics with S*, Fourth Edition (Springer).
28. Hijmans, R.J. (2015). Raster: geographic analysis and modeling with raster data. R package version 2, pp. 3–40.
29. Urbanek, S. (2015). Png: read and write PNG images. R Version 0, pp. 1–7.
30. Brenning, A. (2008). Statistical geocomputing combining R and SAGA: the example of landslide susceptibility analysis with generalized additive models. In *SAGA – Seconds Out*, J. Boehner, T. Blaschke, and L. Montanarella, eds. (Hamburger Beiträge zur Physischen Geographie und Landschaftsökologie), pp. 23–32.

STAR★METHODS

KEY RESOURCES TABLE

REAGENT or RESOURCE	SOURCE	IDENTIFIER
Chemicals, peptides, and recombinant proteins		
Hexane	Sigma, https://www.sigmaaldrich.com/catalog/substance/hexane861811054311?lang=en&region=ZA&gclid=CjwKCAjwmv-DBhAMEiwA7xYrdwnNIhniCxsQt64kAHM7gBUanket8YWRTQB0-LtqnqGq11InEhVntxoCXWsQAvD_BwE	Cat#208752
Deposited data		
All raw data related to this paper	This paper	https://doi.org/10.17632/w6zz33hwz8.1
Experimental models: organisms/strains		
<i>Wachendorfia paniculata</i>	²⁰	N/A
Software and algorithms		
R [27] version 3.4.1	²¹	https://cran.r-project.org/bin/windows/base/
Adobe Illustrator CC	²²	https://www.adobe.com/africa/creativecloud/plans.html?filter=design&plan=individual&promoid=TKZTLDFL&mv=other
Other		
Quantum dots, green (550nm) with zinc oleate ligands	UbiQD, Los Alamos, USA, distributed by Strem: https://www.strem.com/catalog/family/Quantum+Dots/	CAT#298500
Quantum dots, yellow (590nm) with zinc oleate ligands	UbiQD, Los Alamos, USA, distributed by Strem: https://www.strem.com/catalog/family/Quantum+Dots/	Cat#298510
Quantum dots, red (650nm) with zinc oleate ligands	UbiQD, Los Alamos, USA, distributed by Strem: https://www.strem.com/catalog/family/Quantum+Dots/	No longer in production. Closest is Cat#298530
3D-printed quantum dot excitation box	²³	https://doi.org/10.1111/2041-210X.13155

RESOURCE AVAILABILITY

Lead contact

Further information and requests for resources should be directed to and will be fulfilled by the Lead Contact, Bruce Anderson (banderso.bruce@gmail.com)

Materials availability

This study did not generate new unique reagents.

Data and code availability

The datasets generated during this study are available at Mendeley data: <https://doi.org/10.17632/w6zz33hwz8.1>.

EXPERIMENTAL MODEL AND SUBJECT DETAILS

Wachendorfia paniculata is a cormous perennial plant species in the Haemodoraceae family.²⁰ The genus consists of four species, all of which are endemic to the Cape Floristic Region, South Africa.²⁰ All four species produce paniculate floral displays of yellow to

apricot colored flowers.²⁰ These displays are all dimorphically enantiostylous, meaning that the style can be deflected either to the left or the right of the flower and that each plant comprises a single morph.¹⁷ The flowers of all species have three anthers, one on the same side as the style and two which are deflected to the opposite side.²⁰ Helm and Linder²⁰ recognized three different forms of *W. paniculata*. We worked on the most common and variable form which occurs throughout the entire of the species (the other two forms have comparatively restricted ranges). In most populations, the morph ratios of left- and right-handed *W. paniculata* flowers are close to 1:1, suggesting a high prevalence of disassortative mating and low clonality or asexual reproduction.^{16,17} Left- and right-handed *W. paniculata* morphs are fully cross compatible, however selfing lowers seed set compared to outcrossing.¹⁷ *W. paniculata* is commonly seen flowering *en masse*, after fires, which are an important part of the region's ecology.²⁰ *W. paniculata* flowers between August to December and each flower only lasts a single day.²⁰ We conducted all experiments on Stellenbosch mountain (33°56'47.3"S 18°52'50.0"E), Western Cape, South Africa between October and December 2016.

METHOD DETAILS

Quantum dot application

We labeled pollen grains with quantum dots following the methods originally described in Minnaar and Anderson.²³ Pollen grains were labeled with heavy-metal-free CuInSe_xS_{2-x}/ZnS (core/shell) quantum dots (UbiQD, Los Alamos, USA) with zinc oleate ligands (zinc complex with oleic acid) dissolved in hexane (5mg/mL). The q-dot-hexane solution was applied in doses of 0.3μl of per individual dehisced anther using a micropipette with extra-long pipette tips (Lasec 0.1–10μl tips: P2TIP025C-000010). We previously demonstrated that this protocol resulted in ca. 97% of grains in an anther being labeled with q-dots. To distinguish the anther-origin of pollen grains, we used three different q-dot colors to label pollen grains namely, green (550nm), yellow (590nm), red (650nm).

Q-dots fluoresce under UV light excitation. We viewed and identified q-dot labeled pollen grains on stigmas and bees using a standard dissection microscope and 3D-printed quantum dot excitation box.²³

Pollen placement on pollinators

We labeled pollen grains from each of the three anthers of a left- or right-handed *W. paniculata* flower a different color (colors were randomly assigned to anthers) and presented it to foraging honeybees (*Apis mellifera capensis* Eschscholtz, 1822) and carpenter bees [*Xylocopa caffra* (Linnaeus, 1767)] at the end of a 1.5 m wooden stick. Once a bee visited the quantum-dot labeled flower, they were captured and killed using a modified butterfly net²⁴ that allowed us to capture bees without contact between them and the net (which may cause pollen to be displaced). Bees were immediately pinned with a single needle through the center of the thorax onto a foam board and stored at –20°C to preserve them for pollen mapping. We captured 19 carpenter bees (8 L; 11 R) and 19 honeybees (11 L; 8 R).

To map pollen on bee bodies, we created a master body plan, including body segments and wing venation (Figure 2) for carpenter bees and honeybees from photos of several individuals. Then, for each individual bee, we scaled the master body plan to match that particular bee by taking measurements of the length and height of the main parts of the body: wings, legs, abdomen, thorax, and head. Because bees died in various positions, we standardized wing and leg orientation as shown in Figure 2. We then viewed each bee under UV excitation using the quantum dot excitation box as described in Minnaar and Anderson.²³ Each individual quantum-dot labeled pollen grain was mapped as accurately as possible onto its corresponding position on the individually scaled bee-body map. Pollen grains from different anther positions were mapped in different colors. Individual body maps were anchored at the center of the thorax which represented the origins of the x-y axes allowing standardized extraction of the x-y coordinates of each individual pollen grain. We used this mapping approach, because it required the least amount of handling, mitigating post-capture pollen movement and loss of quantum dot labeled pollen grains.

Pollen movement

We used quantum dots to label pollen of three focal plants of the same morph, each with three flowers, within a 50 m² plot. As before, we labeled pollen from each anther a different color. Pollen grains were labeled in the morning and all stigmas within the plot (including those from donor plants) were collected at sunset and frozen for subsequent pollen counting. Donor flowers were removed from the experimental plot at the end of the day. A single pollen movement replicate therefore consisted of three donor plants (9 flowers) of either L or R morphs and all recipient flowers within a 50 m² plot. The position of the plot was randomized for each replicate. Since flowers of *W. paniculata* last for one day only¹⁷ (except during cold and rainy weather), we allowed at least one day's break between pollen movement experiments to reduce the probability that pollen remaining on plants or bee bodies from previous experiments could be transferred to flowers in subsequent experiments. We repeated pollen movement experiments four times for each morph. Since the proportion of left- and right-handed recipients varied among replicates, we standardized overall anther-level pollen receipt for each morph across replicates by adjusting receipt proportions to reflect a 50:50 ratio of left and right recipient stigmas.

We determined ratios of geitonogamous- to outcross-pollen transfer by placing three plants with five flowers each within the population for a day. All pollen on a single plant was labeled using one of three colors so that we could distinguish geitonogamous pollen from outcrossed pollen and thus determine relative contributions of pollen movement within plants. We repeated these experiments twice for each morph resulting in self-pollen transfer rates for 12 plants and 60 flowers. Rates of geitonogamous-pollen transfer were similar between days so we pooled data from different days and calculated self-pollen transfer rates at the level of the plant.

Stigma and anther positions

We picked flowers during peak pollinator activity (9:00–12:00) and measured the absolute distances between anthers, stigmas. We also measured the distance between the center point of the two nectar apertures in relation to their relative positions in the horizontal (x) and vertical (y) plane. The receptive area of the stigma is found at the very tip of the style and is less than 1mm in diameter. To measure the positions of the reproductive parts, we positioned the anthers and stigma of a flower to make contact with a small piece of glass and marked their contact positions, as well as the center point of the two nectar apertures when viewed directly from above on the piece of glass. We converted x and y distances to coordinates by using the center point of the two nectar apertures as the origin and making the x axis parallel to the intersection between the two lower anthers.

QUANTIFICATION AND STATISTICAL ANALYSIS

All analyses were performed using R²¹ version 3.4.1 (R Development Core Team 2017) and the packages nlme²⁵ and multcomp.²⁶

Pollen placement on pollinators

We created body maps and mapped pollen to scale in Adobe Illustrator CC²² and subsequently extracted coordinates for each individual pollen grain for analysis. We then reversed the sign of the x coordinates of all pollen grains from left-handed morphs so that pollen placement could be analyzed according to anther (i.e., upper, lower-opposite, and lower-stigma-side). We tested for differences in pollen placement of each anther on honeybees and carpenter bees on the x and y axis separately using linear mixed-effects models with bee individual as a random factor. We compared pollen placement among anther types using Tukey post hoc comparisons. Replication descriptions can be found in method details.

Pollen movement

To test whether between-morph pollen transfer differed from 66.7% predicted from the 2:1 anther arrangement, we manually computed a chi-square test on all pollen movement data pooled with 66.7% pollen movement between morphs as the expected contingency table frequencies.

Pollen placement heatmaps

We reclassified pollen in pollen-placement maps as between- or within-morph based on the flower origin and the side of the pollinator that the pollen grain was found. For example, a pollen grain on the left side of a pollinator facing the flower was classified as a within-morph pollen grain if it originated from a left-handed flower (i.e., the pollen grain is on the same side as its donor's stigma) and between-morph if it originated from a right-handed flower (i.e., the pollen grain is on the side opposite to its donor's stigma). Because we had unequal sample sizes for left- and right-morph pollen placement for both bee species, we changed the sign of x coordinates of pollen grains so that between- and within-morph pollen placement could be combined for both morphs and mapped on one side of bee bodies. We computed two-dimensional kernel density estimates of between- and within-morph pollen on carpenter bee and honeybee bodies at a 0.1 mm² grid resolution. Density values in these maps were rescaled so that maximum density estimates matched actual pollen counts sampled from 0.5 mm² grid cells overlaying pollen placement maps. We removed rescaled density values < 1 and classified these cells as having no pollen. After computing between- and within-morph pollen density estimates for carpenter bees and honeybees, we calculated a pollen quality–quantity index for each grid cell as the ratio of between- to within-morph pollen, multiplied by the total number of grains found in each grid cell. This created an overall heatmap of pollen quantity and quality across pollinator bodies. Kernel density estimations and heatmaps were computed in R (packages: MASS,²⁷ raster,²⁸ png,²⁹ RSAGA³⁰).

Stigma and anther positions

We determined the positions for anthers and stigmas for 20 flowers of each morph. We tested for differences in the positions of each anther and stigma using linear mixed-effect models with plant identity as a random factor. We compared stigma anther positions using Tukey post hoc comparisons.